7

Nonlinear Transport Through Ultra Narrow Zigzag Graphene Naoribbons

Hosein Cheraghchi
Damghan University
Iran

1. Introduction

Graphene, a monolayer of a honeycomb lattice of carbon atoms has been attracted a great amount of attention from both experimental and theoretical points of view Novoselov et al. (2006). Flat structure of graphene makes its fabrication more straightforward than carbon nanotubes. Moreover, dreams of carbon nanoelectronic approach to the reality based on planar graphene structures. This structure overcomes some difficulties of nanoelectronics based on carbon nanotubes, by using lithography, one-dimensional ribbon patterns on graphene sheets Liu et al. (2009). Experiments in graphene-based devices Ozyilmaz et al. (2007) have shown the possibility of controlling their electrical properties by the application of an external gate voltage. For achieving realistic nanoelectronic applications based on graphene nanoribbons (GNR), width of ribbon have to be narrow enough that a transport gap is opened Han el al. (2007); Li et al. (2008); Wang et al. (2008). Using a chemical process, sub-10 nm GNR field-effect-transistors with very smooth edges have been obtained in Ref.[Li et al. (2008); Wang et al. (2008)] and demonstrated to be semiconductors with band-gap inversely proportional to the width and on/off ratio of current up to 10^6 at room temperature. By connecting GNRs with different types of edges and widths, it is applicable to fabricate electronic devices based on graphene nanoribbons.
The origin of transport gap which is opened in a gate voltage region of suppressed nonlinear conductance is still not well understood Molitor et al. (2009); Son et al. (2006); Sols et al. (2007). Two factors are responsible for transport gap: the edge disorder leading to localization Mucciolo et al. (2009) and the confinement Nakada et al. (1996); Brey & Fertig-a (2006); Bery&Fertig-b (2006); Zheng et al. (2007); Malysheva& Onipko (2008). However, in nonlinear regime, transport gap is also opened by transition selection rules which originates from the reflection symmetry Duan et al. (2008).
Based on the tight-binding approach, GNRs with armchair shaped edges are either metal or Semiconductor Son et al. (2006); Nakada et al. (1996); Brey & Fertig-a (2006); Bery&Fertig-b (2006); Zheng et al. (2007). Moreover, in this approach, zigzag edge ribbons are metal regardless of their widths Malysheva& Onipko (2008). While *ab initio* calculations Son et al. (2006) predict that regardless of the shape of the edges, GNRs are semiconductor. In zigzag GNRs, the bands are partially flat around the Fermi energy, which means that the group velocity of conduction electrons is close to zero. Their transport properties are dominated by edge states.
Similar to carbon nanotubes, electronic transition through a ZGNRs follows from some selection rules. The rotational symmetry of the incoming electron wave function with respect

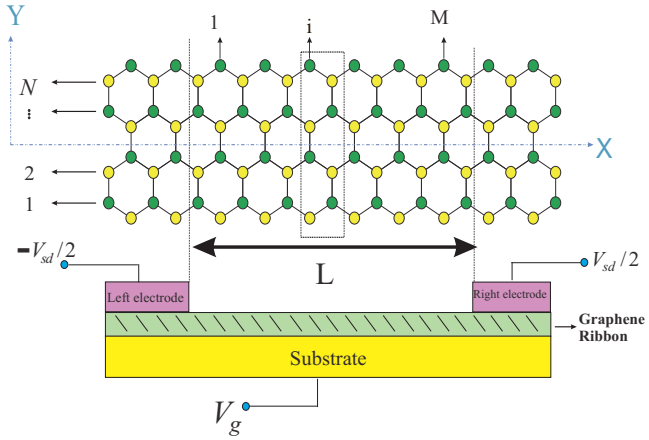

Fig. 1. Gated Zigzag graphene nanoribbon which is divided into three regions: left, right and central region. Dotted rectangular is the unit cell which is used for finding the band structure of graphene ribbons. Lower panel shows a field-effect transistor structure based on graphene ribbons where the gate voltage is applied on the whole system.

to the tube axis is conserved while passing through nanotubes Farajian& Esfarjani& Kawazoe (1999). Correspondingly, the transverse reflection symmetry of the incoming and outgoing wave functions results in the parity conservation in ZGNRs with even number of zigzag chains Duan et al. (2008); Cresti et al.-a (2008); Cresti et al.-b (2008); Akhmerov et al. (2008); Nakabayashi et al. (2009); Wakabayashi& Aoki (2002); Wang et al. (2008). As a consequence of the even-odd effect, a negative differential resistance (NDR) region appears in the I-V characteristic curve of P-N even ZGNR junctions Wang et al. (2008). However, in experiment, edges of graphene ribbons can simply absorb some chemical compounds Kobayashi et al. (2006). Even any small asymmetry is enough to destroy the blocked transitions induced by the parity conservation rule. Although there is no parity selection rules in armchair GNR's, NDR also can be found in their I-V characteristic curves. Such NDR originates from the interaction between the narrow density of states of the doped leads and the discrete states in the scattering region Ren et al. (2010). NDR has also been observed in GNR nanojunctions which its NDR's origin is traced back to the electrostatic profile. Enhanced localization of the HOMO and LUMO states induced by a charge depletion reduces overlap of states and current Cheraghchi& Esfarjani (2008). A NDR behavior has been also reported in P-N nanotube junctions Farajian& Esfarjani& Kawazoe (1999). Historically, NDR was first observed in the degenerated N-P diode junctions Esaki (1958). Nowadays, NDR has been reported in many other molecular devices Dragoman et al. (2007); Cheraghchi& Esfarjani (2008); Cheraghchi& Esmailzadeh (2010). To shed light on the experimental work in Ref.[Li et al. (2008); Wang et al. (2008)] and also introducing new origin of transport gap, in this chapter, we investigate nonlinear transport through ZGNRs by using non-equilibrium Green's function (NEGF) approach. The on/off ratio of the current in the NDR region for gated even ZGNR's reaches up to 10^6. It is also shown that a stable NDR against electrostatic interaction up to 10^5 is appeared in ultra narrow odd ZGNRs around $\pm 1V$ in both positive and negative polarity. These NDRs

are induced by transport gaps which are opened by two selection rules governing electron transition through ZGNRs: (i) the parity conservation, and (ii) that allowed transition are between connected bands Cresti et al.-a (2008); Cresti et al.-b (2008). Based on band structure analyzing, we show that transport gap opened by the second selection rule is filled for ribbons wider than $10nm$. So, sub-$10nm$ ribbons with long enough length provide experimental manifestation of the NDR phenomenon in I-V curve of GNRs. On the other hand, the gate voltage regulates the current flow by shifting the blocked energy regions with respect to the Fermi level. Moreover, for gated even ZGNRs, on/off ratio of the current displays a power law behavior as a function of ribbon length as $M^{7.5}$. However, on-off current ratio for odd ZGNRs increases exponentially with the ribbon length.

This NDR is still robust against edge impurities when the edges are doped by slightly amount of impurity. These edge impurities can significantly affect the electronic structure and transition selection rules of even ZGNRs. Edge states with energies about -0.1 to $0.2eV$ have been observed Kobayashi et al. (2006).

Our calculations show that the details of the electrostatic potential profile along the ribbon can not affect the emergence of NDR. The same conclusion has been reported by Ref.[Wang et al. (2008)], but they have not elaborated on the physical reason behind this robustness. By following the self-consistent charge and potential profiles at different voltages, we demonstrate that at low voltages, strong screening of the external potential at contacts results in a flat electrostatic potential along the ribbon. Subsequently, the e-e interaction at a mean field level, does not change the magnitude of I_{on}. However, for voltages higher than the NDR threshold V_{on}, the transfer of charge along the edges, leads to more reduction in I_{off} which improves the switch performance.

This chapter is organized as follows: in section 2, we briefly explain transition selection rules in symmetric and asymmetric ZGNRs which govern transport properties of GNRs. In section 3, we present Hamiltonian and a short review of NEGF. The origin of NDR seen in the I-V curve of even and odd ZGNRs is explained in section 4. We demonstrate in section 5 that the e-e interaction does not have a significant effect on the phenomena of NDR in the I-V curve. The last section concludes our results.

2. Transition rules

2.1 Transition selection rules in symmetric ZGNR

Presence of the reflection symmetry in the incoming and outgoing wave functions leads to the transition selection rule which regulates the current flow through ZGNRs Duan et al. (2008); Wang et al. (2008). However, there is no reflection symmetry in ZGNRs with odd zigzag chains along the width while even ZGNRs have a mirror symmetric plate which bisects the ribbon plane (Fig.(1)). By application of the symmetry operator on the wave function of even ZGNRs, odd or even parity can be realized for each subband.

$$P\psi_{n,k_x}(x,y) = \psi_{n,k_x}(x,-y) = \eta\psi_{n,k_x}(x,y) \tag{1}$$

where P is the parity operator and ψ_{n,k_x} is the eigen function of n^{th} subband with the wave vector k_x along the longitudinal direction. The eigenvector contains two parts: a plane wave ($e^{ik_x x}$) along the longitudinal axis, and a constraint solution along the transverse direction with free boundary condition. So the eigenvector can be shown as $e^{ik_x x}\phi_n(y)$ Rainis et al. (2009). Eigenvalues of the parity operator are as $\eta = (-1)^{n+1}$, where $n = 1, 2, ..., 2N$ counts bands from the bottom to the top of the band structure, respectively. Eigenvalues of the parity

operator are independent of the value of k_x. As an example, in even ZGNR, lower subband of two central bands has negative parity and upper one has positive parity (Fig.2).
Using the tight-binding approximation, eigenvectors and eigenvalues of the ribbon is derived by diagonalization of the following Hamiltonian Ezawa (2006):

$$\begin{aligned} H\psi_{n,k_x}(x,y) &= E(n,k_x)\psi_{n,k_x}(x,y) \\ H &= H_0 + V_{0,+1}e^{ik_x x} + V_{0,-1}e^{-ik_x x} \end{aligned} \tag{2}$$

where H_0 is the tight-binding Hamiltonian of the unit cell shown in Fig.(1.a). In the nearest neighbor approximation, $V_{0,+1}, V_{0,-1}$ are the overlap matrices between the marked unit cell ('0') and its left ('-1') and right ('+1') unit cells. Having eigenvalues of this Hamiltonian $E(n,k_x)$ results in the energy spectrum of graphene ribbons.

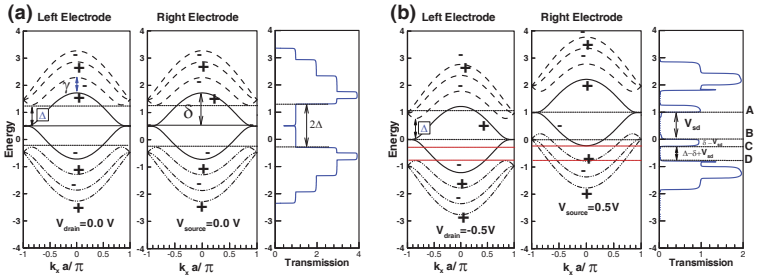

(a) (b)

Fig. 2. transmission (right panel) and band structure of right (center panel) and left (left panel) electrodes for ZGNR with 6 unit cells in length and 4 zigzag chains. Applied bias is considered to be **a)** $V_{\rm sd} = 0$ and **b)** $V_{\rm sd} = 1.0V$. Gate voltage is $V_g = 0.5V$. Here, $\triangle$ and γ are the energy separation of upper/lower group of bands from the central bands at the Dirac point ($k_x = \pm 2\pi/3a$) and $k_x = 0$, respectively. Moreover, δ is the half-width of the central bands at $k_x = 0$.

As a consequence of Eqs.(1,3), in even ZGNRs, we have $[P, H] = 0$. Therefore, parity is conserved during coherent transport. Parity conservation in even ZGNRs results in the blocked transition of the incoming wave function with positive parity into the outgoing wave function with negative parity of the central subbands.
Electronic transition is controlled by two selection rules. First, the parity is conserved in tunneling of electron through even-ZGNRs. Therefore, at zero source-drain voltage, one can expect full transmission which is shown in Fig.(2.a). In this case, all bands with the same parity are energetically aligned and there is no gap in the transmission curve. In Fig.(2.a), the energy of transmission curve is shifted by the gate voltage ($0.5V$). Parity of each band is indicated by plus/minus signs. In the range of 2Δ, there is one conducting channel which results in unit transmission coefficient.
Fig.(2.b) represents band structures of electrodes which are shifted with respect to each other due to the source-drain voltage $V_{\rm sd} = 1.0V$. The gap in the transmission curve of Fig.(2.b), AB region, indicates that transport between bands of opposite parity is blocked. In the energy regions in which back scattering of electrons increases due to the selection rules, it is established that the transmission decays exponentially with the length as $e^{-\gamma L}$.

The second selection rule which governs electron transport through ZGNRs, is that, electron transition is allowed between connected bands. Figs.(2.a,b) show the band structure classified in three different groups; namely, central, upper and lower bands which are indicated by solid, dashed and dashed-dot-dot lines, respectively. The common feature of bands in each group is that, they are connected at the zone boundary, while distinct groups are disconnected. When one considers the electron transport, the longitudinal momentum k_x, of electrons changes as a result of applied $V_{\rm sd}$. The precise form of this variation in k_x, crucially depends on profile of the superimposed longitudinal potential. These groups are disconnected from each other from the point of longitudinal momentum. Variation of momentum of electron k_x depends on the shape of superimposed longitudinal potential. The transport properties for smoothly varying $V_{\rm sd}$, are significantly different from $V_{\rm sd}$ profiles with sharp spatial variations. The electronic transition between an eigenstate (m_1, k) in the right electrode and an eigenstate (m_2, q) in the left electrode is proportional to Fourier transform of longitudinal voltage and structure factor Cresti et al.-a (2008); Cresti et al.-b (2008),

$$\langle \psi_{m_1}(k) \mid V_{sd}(x) \mid \psi_{m_2}(q) \rangle = S\tilde{V}_{sd}(k-q), \tag{3}$$

where structure factor of S is equal to $[1 + (-1)^{P_{m_1}+P_{m_2}}]$ for even ZGNRs and parity of band m is equal to $P_m = (-1)^{(m+1)}$. Parity selection rule in even ZGNRs originates from this structure factor. This parity selection rule is mesoscopic analogue of chirality factors governing transport of Dirac electrons in planar graphene Ulloa& Kirczenow (1987).

If a constant gate voltage is applied on the whole system, since there is no longitudinal potential variation, momentum of electron remains unaffected against the gate voltage. However, linear variation of the applied source-drain bias (with the slope $V_{\rm sd}/L$) changes the electron momentum. So, smooth variation of the potential in longer ribbons results in a small momentum variation of electron. Consequently, transition of electron between disconnected bands is forbidden when the length of ribbon is so large that one can assume $\tilde{V}_{sd}(k-q) \rightarrow \delta(k-q)$. Therefore, a smooth potential in the longitudinal direction can just scatter the electron among the class of states belonging to the same group of connected energy bands.

Now let us focus on the two transport gap regions: AB and CD in Fig.(2.b). The AB gap is a consequence of parity selection rules, while the CD gap is due to blockage of transition between disconnected groups. As can be seen in Fig.(2.b), the AB gap is proportional to the source-drain voltage, V_{sd}. Moreover, this gap is independent of the ribbon width. Of course, in the wide ribbons, the upper and the lower band groups approach to the central group, especially at the point $k_x = 0$, where γ in Fig.(2.a) tends to zero as log-normal.

When the ribbon width is increased, the separation γ between the upper/lower and central groups of bands, is reduced, which tends to loosen the second selection rule based on band groups; hence filling in the gaps. However when we increase the ribbon length, our classification of bands into connected groups is recovered. Therefore the AB gap is essentially governed by the aspect ratio of ZGNR.

The CD gap is equal to $\Delta - \delta + V_{\rm sd}$, where Δ and δ are the energy separation of upper/lower group from the central bands at the Dirac point, and the half width of the central bands at $k_x = 0$, respectively. The dependence of Δ on width N is: $\Delta \propto (2.13 \pm 0.02)N^{-(0.864\pm0.003)}$, while δ has a Log-Normal behavior which asymptotically approaches to the constant value of 0.9738 ± 0.0002 as N goes up to 10. The conducting region BC in Fig.(2.b) can exist only, when $\delta - \Delta < V_{sd} < \delta$. From the dependence of Δ and δ on N, the CD gap exists if N is less than 30. Hence, NDR is estimated to be observable for ribbon width $\leq 7nm$. The lowest

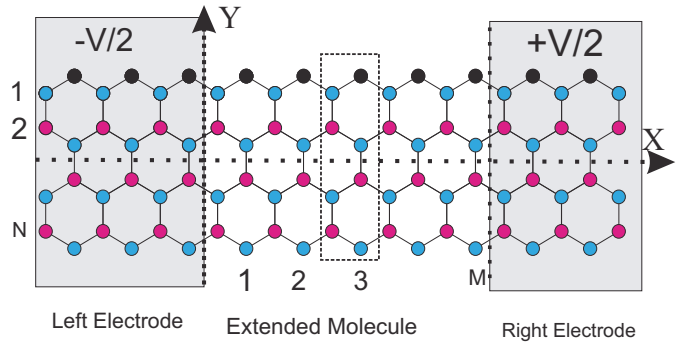

Fig. 3. Even asymmetric zigzag graphene nanoribbon considered as a central region attached to two electrodes. Transverse zigzag carbon chains and unit cells inside the central region are labeled by N and M. Darker edge atoms are absorbed atoms which make ribbon asymmetric in respect to the X-axis.

achieved ribbon width is sub-10nm-wide ($\sim 2 \pm 0.5nm$) Li et al. (2008); Wang et al. (2008) with the length $\sim$ 236nm. Such long ribbons with small width provide fascinating experimental manifestation of the selection rules in transport properties.
One of the experimental requirements of the nanoribbon fabrication is the presence of some absorbed edge impurities. So, reflection symmetry could be simply failed during designing of electronic devices based on ZGNRs. Operation of an electronic device should not be affected by small asymmetry. Recently Wang et al. (2008), based on even ZGNR substrate and also the parity selection rule, an N-P diode junction was designed. This diode shows an NDR in positive polarity of its I-V curve. According to the previous discussions, this device is strongly sensitive to any asymmetry. Electronic devices designed by the transition rule arising from disconnecting band groups is much reliable than those which are based on the symmetry. In the next section, we introduce a nanoswitch which its operation is not so sensitive to the asymmetry. Fig.(3) shows asymmetric zigzag graphene nanoribbon with even number of zigzag chains in width (N).

2.2 Transition selection rules in asymmetric ZGNR

Those selection rules controlling the electron transition through even ZGNRs will be modified when impurity absorption changes onsite energies of atoms located in one edge of the ribbon. Application of the edge asymmetry influences the selection rules as the following:
1) Transition between those subbands which have been already forbidden based on the parity conservation, would be now allowed.
2) As shown in Fig.(4.b), in the spectrum of central bands of even ZGNRs, an energy gap is induced by the edge impurity. The opening of the gap depends directly on the onsite energy attributed to the edge impurity. As a result, in this case, the first conduction and the last valance bands detach from each other so that they do not belong to the same band group. Therefore, transition between these subbands is not allowed now.

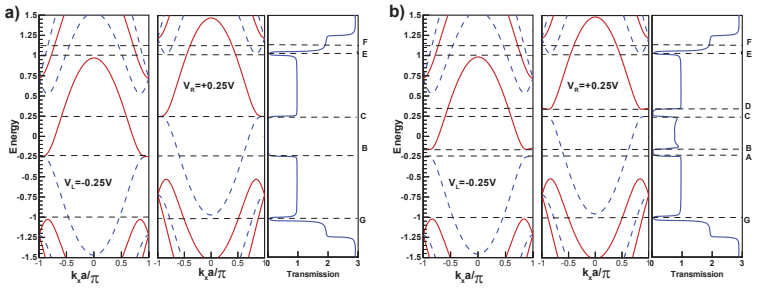

(a) a (b) a

Fig. 4. Energy spectrum of the left and right electrodes of graphene ribbons with 4 zigzag chains $(M, N) = (12, 4)$ under $0.5V$ applied bias a) without b) with the presence of the edge impurity. In figure (b), it is supposed that the doping impurities adsorbed by one of the ribbon edges can induce additional onsite energy on the edge atoms as $\varepsilon_\alpha = 0.1$. To investigate the selection rules, transmission also is plotted. Bands with solid and dashed lines have positive and negative parity, respectively.

These two selection rules have two opposite operations so that depending on the system length and edge impurity, they compete with each other. One of them increases transmission and the other one decreases it. Fig.(4.b) shows the energy spectrum and transmission through a ZGNR (with $N = 4$) at the applied bias of $0.5V$. It is supposed that the edge impurity changes onsite energy of the edge atoms as the value of $\varepsilon_\alpha = 0.1$. The energy gap induced by the edge impurities also keeps its trace in the transmission curve. Due to the asymmetry-induced gap, transmission in the energy ranges of AB and also CD shown in Fig.(4.b) is zero. However, one conducting channel is allowed in the energy range of DE. The only allowed transition in this energy range is the transition from the first conduction band of the right electrode to the same band of the left electrode. The same as symmetric case, at the energy points corresponding to E and G, the flow of the current is blocked due to the transition between two different band groups. By application of the edge impurity, it is interesting to note that in the energy range of BC, one conducting channel is opened and contributes into the transport. According to the parity selection rule, in this energy range, the electronic transition even ZGNRs must be blocked. However, parity is not conserved in asymmetric even ZGNRs and the transition is permissive. On the other hand, because of the asymmetry-induced energy gap, from the viewpoint of longitudinal momentum, the upper band of central group belonging to the left electrode is detached from the lower band of the central group belonging to the right electrode. So, the electronic transition between detached bands is forbidden. As it was explained in the previous section, if the ribbon length is long enough, the electron transition between these two detached subbands is effectively blocked. However, if the system length is considered to be very short (e.g. M=1), the transition between disconnecting bands is permissive. In the ribbons shorter than a critical length, application of the asymmetric edge impurity can not effectively destroy the parity conservation. As shown in Fig.(5.a), the parity conservation however gradually fails when the ribbon length approaches the critical length. Therefore, in the energy range of $B - C$, transmission increases with the ribbon length. On the other hand, in a ribbon longer than the critical length (here $M_{cr.} = 12$), transition of electrons between the separated central bands belonging to the different electrodes is gradually blocked

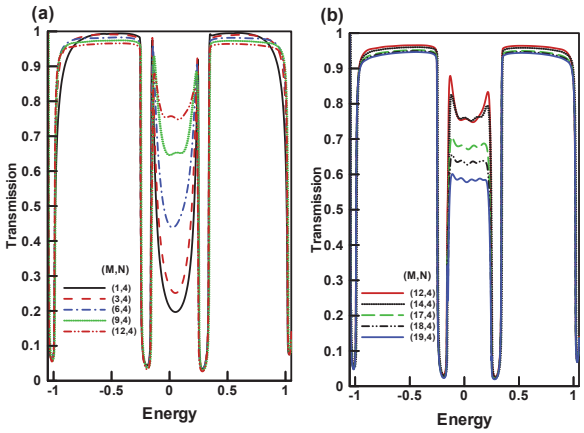

Fig. 5. Transmission through graphene ribbon with 4 zigzag chains in width for different ribbon lengths: a) $M \leq 12$ b) $M \geq 12$. Applied bias is considered to be $0.5V$. Edge impurity changes onsite energy of the edge atoms as $\varepsilon_\alpha = 0.1t$.

and so transmission in Fig.(5.b) decreases with the length. Based on this competition between two selection rules, one can explain non-linear transport through asymmetric even ZGNRs.

3. Hamiltonian and formalism

Fig.(1) shows schematic side view of graphene nanoribbon. In presence of source-drain applied potential, ribbon is divided into three regions; left, right electrodes and also central interacting region. Gate voltage is applied by means of substrate on the graphene plate. The interacting Hamiltonian is written in the tight-binding approximation. This Hamiltonian is a functional of charge density:

$$H\{n\} = \sum_i (\varepsilon_i + [(x_i - x_0)/L - 0.5]V_{sd} + \sum_j U_{ij}\delta n_j])c_i^\dagger c_i + \sum_{<ij>} t(c_i^\dagger c_j + c_i c_j^\dagger), \quad (4)$$

ε_i shows onsite energy of i^{th} carbon atom and t represents the hopping integral between nearest neighbor atoms. One π orbital is considered per each site for graphene system. Without losing any generality, we set onsite energies (ε_i) of all sites equal to zero. All energies are in units of $t_{C-C} = 2.5eV$. Application of a gate voltage is achieved by shifting atomic onsite energies in all three regions. The applied source-drain potential, V_{sd}, and the gate voltage, V_g, preserve transverse symmetry with respect to the ribbon axis (X direction in Fig.(1)). Linear variation of the source-drain voltage along the ribbon is the solution of the Laplace equation with Dirichlete boundary condition on the contacts. U_{ij} is the electrostatic Green's function and $\delta n_i = n_i - n_i^0$ is the change in the self-consistent charge n_i from its initial equilibrium zero-bias value. This third term is the direct Coulomb interaction created by the bias-induced charges at a mean field level which is the solution of Poisson equation. The electrostatic Green's function for a distribution of charges between two parallel conducting planes located at $x = 0, L$ which are held at zero potential Jackson (1975), has the following form:

$$U(\overrightarrow{r},\overrightarrow{r'}) = 2\int_0^\infty dk J_0(\alpha k)\frac{\sinh(kz_<)\sinh(k(L-z_>))}{\sinh(kL)},$$
$$\alpha = \sqrt{(x-x')^2+(y-y')^2+U_H^{-2}}, \tag{5}$$

where U_H is the Hubbard parameter whose semi-empirical value for carbon Esfarjani& Kawazoe (1998) is about $4t_{C-C}$. This parameter determines the strength of electron-electron interaction. This electrostatic Green's function is appropriate for the kernel of Ohno-Klopmann model Ohno& Klopman (1964).
For self-containing, we present a very brief review of the NEGF formalism. Charge density in non-equilibrium situation is calculated by $[-iG^<]$ as the occupation number in the presence of the two electrodes with an applied source-drain bias Taylor et al. (2001).

$$n_i = \frac{-1}{\pi}\int_{-\infty}^{E_F-\frac{V}{2}} Im[G^r(E)]_{ii}dE + n_i^{non-eq} \tag{6}$$

where non-equilibrium part of charge can be calculated by the following integral,

$$n_i^{non-eq} = \frac{1}{2\pi}\int_{E_F-\frac{V}{2}}^{E_F+\frac{V}{2}} [-iG^<(E)]_{ii}dE \tag{7}$$

where within a one-particle theory ,

$$-iG^< = G^r(\Gamma_L f_L + \Gamma_R f_R)G^a \tag{8}$$

Here $f_{L/R}$ is the Fermi-Dirac distribution function of electrodes and G^r/a is the retarded/advanced Green's function defining as the following:

$$G^{r/a} = [(E\pm\eta)I - H\{n\} - \Sigma_L^{r/a} - \Sigma_R^{ra}]^{-1} \tag{9}$$

and Γ is the escaping rate of electrons to the electrodes which is related to the self-energies as $\Gamma_p = i[\Sigma_p^r - \Sigma_p^a]$ with $p = L/R$ Munoz (1998); Datta (1995); Taylor et al. (2001). Here $\eta \to 0^+$. Solving equations 6 and 9 self-consistently results in a self consistent charge and Green's functions. Finally, the current passing through the molecule is calculated by the Landauer formula for zero temperature Datta (1995) which is valid for coherent transport.

$$I(V) = \frac{2e}{h}\int_{E_F-V/2}^{E_F+V/2} dE\, T(E,V) \tag{10}$$

where $T(E,V)$ are the bias dependent transmission coefficient.

$$T = \mathrm{Tr}[G^r\Gamma_R G^a\Gamma_L] \tag{11}$$

4. Negative differential resistance

In this section, we will present our results about nonlinear transport properties which emerges in current-voltage characteristic curves.

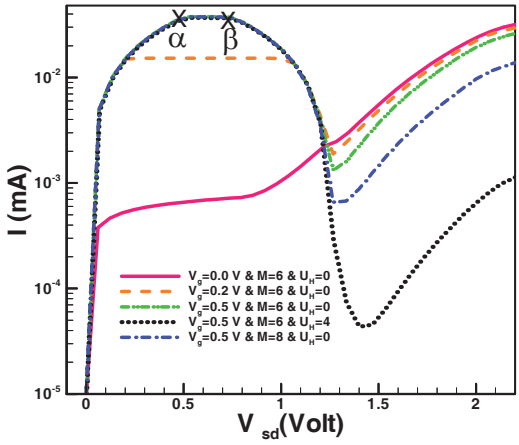

Fig. 6. Current-voltage characteristic curve for different gate voltages when the ribbon size is as $(N, M) = (4, 6)$. The effect of different parameters such as size effect, electrostatic potential and also gate voltage is investigated on I-V curve. Hubbard parameter (U_H) is on site Coulomb repulsive.

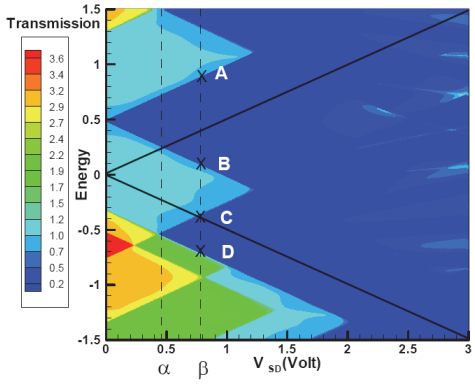

Fig. 7. Contour plot of transmission with respect to the energy and V_{sd} for the system size (N,M)=(4,6) and the applied gate voltage $V_g = 0.5V$. Darked Oblique lines shows the current integration window. Points marked by A, B, C, D correspond to the horizontal lines with the same name in Fig.(2). Lines of α, β are the trace of points with similar names in Fig.(6). Fermi energy was fixed at zero $E_F = 0$.

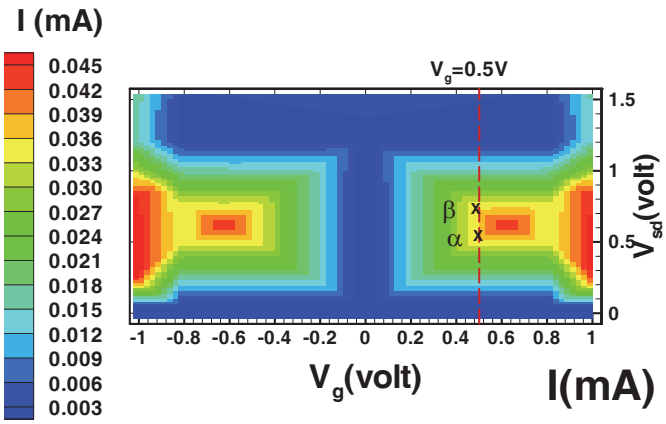

Fig. 8. Contour plot of the current in terms of V_{sd} and V_g for a zigzag graphene nanoribbon with (N,M)=(4,6). Vertical dotted line corresponds to $V_g = 0.5V$. α and β are those points which was shown in Figs(6,7).

4.1 NDR in gated-EVEN zigzag graphene nanoribbon

Fig.(6) shows current-voltage characteristic curve of a ZGNR with 4 zigzag chains and 6 unit cells in length. In the case of zero gate voltage, flow of current is blocked due to the parity selection rule, while at a given $V_{\rm sd}$, gate bias turns the current on. After a range of $V_{\rm sd}$ in which the current remains unchanged, current begins to reduce with increasing $V_{\rm sd}$. NDR threshold voltage $V_{\rm on}$ decreases with gate voltage for $V_g < 0.6V$. Dependence of NDR threshold voltage on the gate voltage can also be seen in Fig.(8). This NDR also symmetrically appears in the negative polarity of $V_{\rm sd}$. The NDR threshold voltage and $I_{\rm on}$ remain unchanged in the presence of the electron-electron interaction (with a given Hubbard term $U = 4t_{C-C}$). However, reduction of the current in off state, $I_{\rm off}$, is intensified when one takes electrostatic potential into account.

To understand the origin of NDR, it is helpful to look at the 3D contour-plot of transmission in plane of energy and $V_{\rm sd}$ which is presented in Fig.(7). Blocked energy intervals AB and CD, which are indicated in Fig.(7), correspond to those intervals shown in Fig.(2). For voltages lower than the vertical line α ($V < V_\alpha$), transmission is a nonzero constant for the whole region of the conduction window represented in Eq.(10). As a result, current increases proportionally to $V_{\rm sd}$. In the voltage interval $[V_\alpha, V_\beta]$, the blocked region AB, originating from the parity selection rule, contributes to the current integration window of Eq.(10). However, nonzero range of transmission remains unchanged along with $V_{\rm sd}$ resulting in the fixed current in the voltage range $[V_\alpha, V_\beta]$. So, current remains unchanged in this range. For voltages $V \geq V_\beta$, the CD gap contributes in the current integration window, and consequently the NDR phenomenon emerges.

Regarding the importance of gate voltage in the current flow, let us investigate the effect of the gate voltage on $I - V_{\rm sd}$ curve by contour plotting of the current with respect to $V_{\rm sd}$ and V_g in Fig.(7). For gate voltages $|V_g| < 0.1V$, shift of transmission is not remarkable enough to contribute to conducting channels in the current integration. So, current is blocked by the

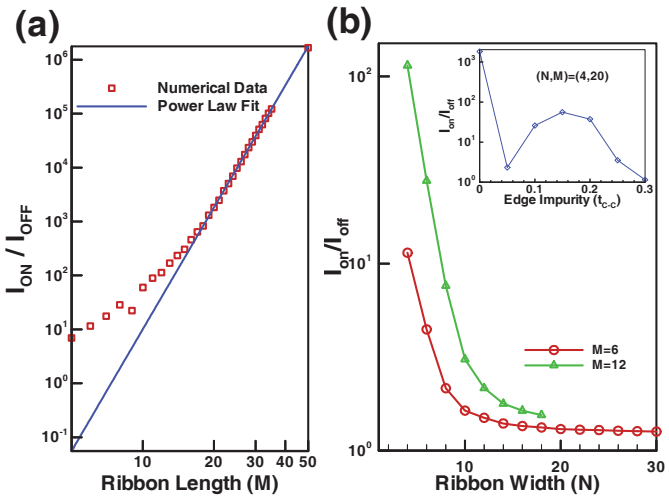

Fig. 9. a) On-off ratio of the current increases as a power law with the ribbon length for $N = 4$ and $V_g = 0.5V$. b) On-off ratio of the current decreases with the ribbon width (circle and triangular points) while it is disappeared for edge impurity (diamond points) stronger than $0.3t_{C-C}$ (inset figure).

parity selection rule. In the range $0.1V < |V_g| < 0.6V$, contribution of conducting region BC in transport is accompanied with the blockage arising from AB and CD gaps in voltages $V > V_{\text{on}}$. As a consequence, current reduces after a threshold voltage. In this range, on/off ratio of the current increases and V_{on} reduces with increasing the gate voltage.

As can be seen in I-V curves of Fig.(6), off current reduces for longer ribbons which enables us to achieve high performance switches by increasing aspect ratio of the ribbon length/width. The reason is connected to smooth variation of the applied potential along the ribbon such that during transport, electrons are scattered among those states which belong to continuous bands. As a consequence, blockage originating from electronic transition between disconnected bands is intensified by increasing the ribbon length. In fact, when the length of ribbon increases, transmission in the AB and CD gaps decreases exponentially.

Since off current is induced by contribution of the gaps in the current integration, I_{off} efficiently decreases with increasing the ribbon length (M). Fig.(9.a) shows that $I_{\text{on}}/I_{\text{off}}$ displays a power law behavior as a function of the ribbon length for large M: $I_{\text{on}}/I_{\text{off}} \propto M^{\eta}$ where $\eta = 7.5061 \pm 0.03505$. As an example, for $M = 50$, on/off ratio goes up to 10^6 which suggests experimental fabrication of high performance switches based on the GNR nanoelectronics.

Experimentally, it was observed in Ref.[Li et al. (2008); Wang et al. (2008)] that the room-temperature on/off ratio induced by the gate voltage increases exponentially as the GNR width decreases. They observed that $I_{\text{on}}/I_{\text{off}}$ is equal to $1, 5, 100$ and $> 10^5$ for $W = 50nm, 20nm, 10nm$ and sub-$10nm$, respectively. Similarly, as shown in Fig.(9.b), on/off ratio calculated for the set up considered in this paper, also decreases with the ribbon width, while reduction of on/off ratio can be compensated by considering longer ribbons. However, NDR phenomenon is disappeared for the ribbons wider than $7nm$.

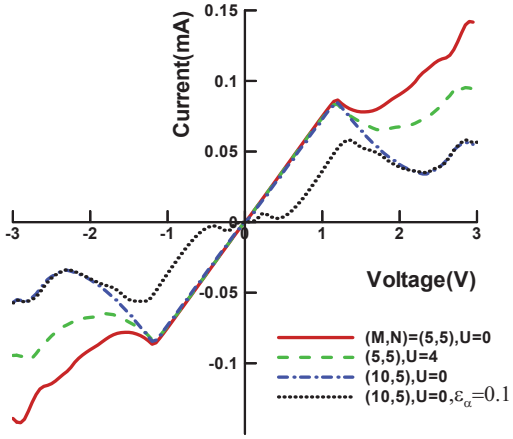

Fig. 10. Current-voltage characteristic curve of an odd zigzag graphene nanoribbon with $N = 5$ (zigzag chains). I-V curves are compared for two ribbon lengths; $M = 5$ and 10. For the case of $(M, N) = (5, 5)$ and for comparison purpose, I-V curve is also plotted in the presence of electron-electron interaction (U). NDR phenomena is preserved when one of the ribbon edges is doped by slight impurity (as ε_α).

In *ab initio* calculations Son et al. (2006), by using hydrogen-termination of zigzag edges, mirror-symmetry of ZGNRs and consequently parity conservation could be retained. Correspondingly, by several repetition of the heat treatments and hydrogenation, it is also possible to create well-ordered H-terminated edges in experiment Kobayashi et al. (2006). However, the edge states with energies about -0.1 to 0.2 eV have been experimentally observed Kobayashi et al. (2006) that emerge at hydrogen-terminated zigzag edges. To simulate the edge states and the effect of symmetry breaking on NDR phenomenon, it is assumed to dope one of the ZGNR edges by slight impurity. Edge impurity is considered to apply as a change in the on-site energy of the edge atoms (ε_α) with respect to on-site energy of the other atoms. In case of edge disorder, ε_α plays the role of the averaged on-site energy of the edge atoms. Inset figure indicated in Fig.(9.b) shows that on/off switching reduces with the edge impurity strength, however, NDR still emerges for $\varepsilon_\alpha < 0.3t_{C-C}$.

4.2 NDR in ODD zigzag graphene nanoribbon

Current-voltage characteristic curve of an odd ZGNR with 5 zigzag chains ($N = 5$) is shown in Fig.(10). Lower than the external bias $1.2V$, current increases linearly with the applied bias as an *Ohmic* device. After a threshold voltage ($1.2V$), NDR occurs at both positive and negative polarity.

The origin of NDR seen in odd ZGNRs is interpreted by analyzing their energy spectrum accompanied to transmission curve. Fig.(11) shows energy spectrum $E(n, k_x)$ and transmission through 5 ZGNR at $V = 1.4V$.

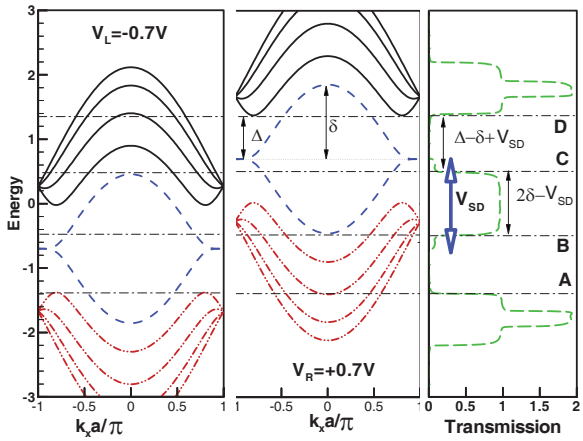

Fig. 11. Energy spectrum of the left and right electrodes and transmission through zigzag graphene nanoribbon with $(M, N) = (10, 5)$ at voltage ($V_{SD} = 1.4V > V_T$). The band structure is divided into three groups which are called by upper , centeral and lower band groups. These groups are classified based on the bands which are connected in terms of k_x. The bold hollow arrows show the current integration window which based on Eq. 10, is proportional to V_{SD}. The Fermi level is set to be as $E_f = 0$. The half-width of the central bands at $k_x = 0$ is called as δ which is equal to the threshold NDR voltage. Δ is energy separation of the upper bands from the central bands at the Dirac points. Transport gaps AB and CD are equal to $\Delta - \delta + V_{SD}$.

In odd ZGNRs, parity has noncommutative relation with the Hamiltonian. Therefore, parity has no conservation and consequently transmission is not blocked by the parity selection rule, while parity conservation in even zigzag nanoribbons opens transmission gap around Fermi level Cheraghchi& Esmailzadeh (2010). In the range of BC of Fig.(11), there exists one conducting channel which results in the unity transmission around the Fermi level. So at low biases, current increases linearly with bias. This single-channel transport around the Fermi level remains unchanged even for high voltages. However, for voltages greater than the NDR threshold voltage ($V > V_T$), blocked regions marked by the ranges of AB and CD comes into the current integration window. The current integration window is proportional to V_{SD} and is shown with the bold hollow arrows in Fig.(11). Therefore, when source-drain applied bias increases, current begins to decrease.
Blocked regions (AB and CD) arise from a selection rule which increases back scattering in the lengthy ribbons. According to this rule, the electronic transition between those bands which are disconnected from the view point of longitudinal momentum, decreases exponentially with the length.
Band structure analyzing demonstrates that the threshold voltage is equal to the half-width of the central bands at $k_x = 0$ as $V_T = \delta = [E(N+1, k_x = 0) - E(N, k_x = 0)]/2$. As shown in Fig.(11), Δ is energy separation of the upper bands from the central bands at the Dirac points. There is a Log-Normal behavior of δ versus number of zigzag chains (N) such that as $N \to \infty$, the NDR threshold voltage asymptotically approaches to the value of 0.9738 ± 0.0002. So the NDR threshold voltage slightly decreases with the ribbon width. Analyzing transport gaps appeared in the band structure shows that they are equal to $\Delta - \delta + V_{SD}$ where $\Delta \propto$

N^{-1}. Since δ approaches to a constant values when $N \to \infty$, in a given voltage, transport gap is disappeared for $N > 30$ which is nearly equivalent to $10nm$. The other effect which enhances performance of this electronic switch, is the ribbon length. Fig.(10) shows an increase of on/off ratio with the ribbon length. Moreover, NDR region ($V_{off} - V_{on}$) occurs in a more extended range of the I-V curve. Exponential decay of transmission with the length in the gap regions develops quality of switching. In odd ZGNRs, I_{on}/I_{off} increases exponentially with the ribbon length.
If one of the ribbon edges is doped by small impurity such as $\varepsilon_\alpha = 0.1t$, because of a band gap which is induced by the edge impurity in low biases, current decreases. Fig.(10) represents that even with the presence of edge impurity, still the region containing NDR still exists. However, asymmetry decreases on/off ratio of the current. Furthermore, asymmetric ZGNR behaves as a semiconductor while symmetric ZGNRs behave as an Ohmic devices Ren et al. (2010). The effect of asymmetry on NDR competes with the ribbon length. Since asymmetry can not be ignored in experiment, longer ribbons are in favor of keeping NDR in the I-V curve. On the other hand, additional to edge impurity, this asymmetry can be assigned to a sublattice symmetry breaking induced by spontaneous ferromagnetic spin ordering of the electrons localized at the zigzag edges Son et al. (2006). In fact, the border atoms at the two opposite zigzag edges belong to different sublattices. So spin orientation along the edges induces different magnetic potentials at the edges. As a result, a small band gap is opened around Fermi level which depending on the ribbon width, is about 0.15 eV. The asymmetry which we have considered is about 0.3 eV which is stronger than the gap opened by spin-polarization of the edges. We can conclude that spin-polarization along the zigzag edges can not affect emerging of this NDR phenomenon Ren et al. (2010).

5. Electrostatic potential and charging effect on NDR

Emerging phenomenon of negative differential resistance in I-V curve is not destroyed by the e-e interaction and is independent of the details of electrostatic potential profile. However, interaction reduces off-current as shown in the I-V curves of Fig.(6). In this section, we present the reason for robustness of NDR against e-e interaction for the gated even ZGNR. The same results can be extracted for odd ZGNRs.
To substantiate the above claim, comparison of transmission curves in the presence and absence of the e-e interaction is useful. It is apparent from Fig.(12.a) that for voltages less than $V_{\rm on}$, transmission in conducting channels is robust against the e-e interaction while transmission increases in the gaps with respect to the non-interacting case. But this enhancement is slight enough which can not affect the emergence of NDR. However, for voltages $V > V_{\rm on}$, interaction lowers transmission coefficient in the conducting channels (such as BC region) in which higher subbands participate in transport. Such behavior is corroborated in Fig.(12.b) which indicates transmission at that voltage corresponding to the off-current, $V_{\rm off}$. Reduction in the transmission coefficient of the conducting channels results in further reduction of the off-current. To explain the reason for such phenomenon, it is necessary to study the potential and charge profiles. Electrostatic potential averaged on each unit cell is represented in Fig.(13.a) in terms of the ribbon length. For voltages less than $V_{\rm on}$, potential sharply drops only at the contact regions which connects the system to electrodes. In such a case, external potential is strongly screened by redistributed electrons and, electrostatic potential of the central atoms remains close to zero. Screening is performed by discharging of electrons from the area connected to the source and their accumulation around the drain electrode. These facts are obvious from transferred charge and electrostatic

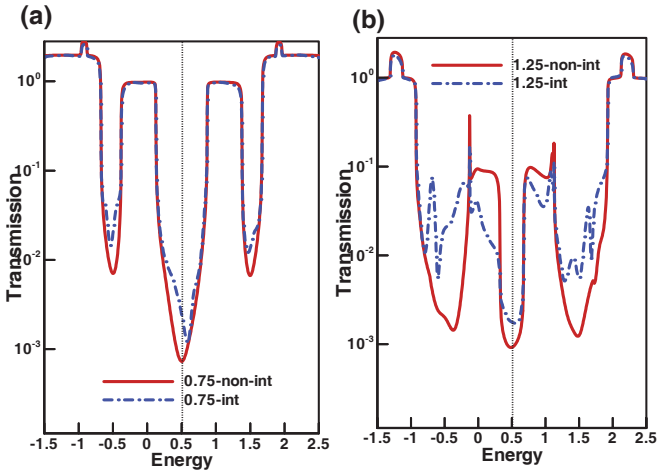

Fig. 12. Transmission curve of zigzag graphene nanoribbon with 4 zigzag chains in width for voltages a) 0.75 volt b) 1.25 volt. Interacting and non-interacting curves are compared with each other.

potential profiles represented in Fig.14. Since $U(n - n_0)$ determines electrostatic behavior of the potential, discharging of electrons weakens the external potential penetrated from the source electrode. Moreover, charge accumulation around the drain electrode prevents potential drop in the central part of the system. So in the case of strong screening, potential drops only at the contacts. However, when the applied bias goes beyond 1 volt, screening is being weakened and external potential can penetrate inside the central region. The reason as to why screening is weak, can be sought in charge distribution. Figure (13.b) illustrates that for voltages less than 0.5 volt, in and out flow of charge are balanced with each other such that the total transferred charge remains close to zero. However, around the voltage V_{on} and voltages above, the charge is mainly transferred from the edges of the ribbon, so that the source electrode does not inject further charge to middle atoms of the ribbon. As a consequence, by increasing the applied bias and so gradient of the potential along the central region, charge depletion is mainly enhanced in the middle bar area of ZGNR. On the other hand, since the only way for transporting electrons is the edge atoms, significant accumulation of charge appears along the two edge lines of ZGNR.

In summary, at voltages less than V_{on}, electrostatic potential is only dropped at the contacts and therefore momentum of electrons is only varying in the area where the potential drops, while longitudinal momentum of electron remains unchanged across the central portion. In other words, potential steeply drops in the low-area district around the contacts which results in violation of the blockage rule which governs on transition between disconnected energy bands. Subsequently, transmission coefficient slightly increases in the blocked energy ranges. In other words, in this case, an increase in gradient of the potential facilitates electronic transport in the blocked energies. Note that interaction preserves transverse symmetry, so the parity selection rule still governs electronic transport. Therefore, the AB gap induced by the parity conservation still survives for voltages larger than V_{on}. For voltages $V > V_{\text{on}}$, electrostatic potential gradually penetrates into the whole system so that the potential of the

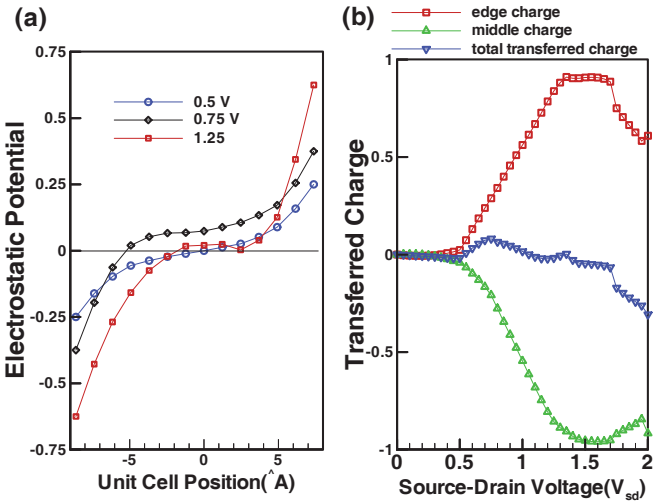

Fig. 13. a) Edge, middle and total transferred charge in terms of source-drain applied bias. b) Electrostatic potential per unit cell in terms of unit cell position for source-drain voltages 0.5, 0.75, 1.25 volts. The gate voltage is for all curves equal to $V_g = 0.5$ V.

central region is not flat. In addition, because the edge transport of electrons dominates, the transverse potential is deeper in the middle of ZGNR than its edges. Therefore, the band structure of the interacting central region differs from the band structure of electrodes. As a consequence, for voltages $V > V_{\text{on}}$, transmission of conducting channels and also off current reduces.

Comparison of odd and even ZGNRs: There are some interesting differences between results arising from *odd* ZGNRs with those results belonging to *even* ZGNRs Cheraghchi& Esmailzadeh (2010) which is kind of odd-even effect. In odd ZGNRs, NDR appears in voltages upper than $1V$ while in even ZGNR, NDR occurs for voltages lower than $1V$. On/off ratio of the current in gated even ZGNRs increases as a power law with the function of the ribbon ribbon length while in odd ZGNRs, on/off increases exponentially. Screening of the external bias by electrons of system in even ZGNRs is so stronger than screening effects in odd ZGNRs. As a consequence, the effect of electrostatic interaction on increase of the on/off ratio in even ZGNRs is much effective than in odd ZGNRs. Furthermore, transferred charge from/into the central portion of graphene nanoribbon depends on odd or even zigzag chains in width.

6. Conclusion

As a conclusion, based on a model calculation and non-equilibrium Green's function formalism, we found that there exists a region of negative differential resistance in I-V curve of ultra narrow (lower than $10nm$) zigzag graphene nanoribbons with odd or even number of zigzag chains in width. In this range of widths, two selection rules govern on the electronic transition are: (i) the parity conservation, and (ii) the allowed transition between connected bands. On/off ratio of the current increases up to 10^5 as a function of the ribbon length which proposes possibility of manipulation of ZGNRs as high quality switch in nanoelectronic based on graphene nanoribbons. Emergence of the NDR phenomenon is not sensitive to

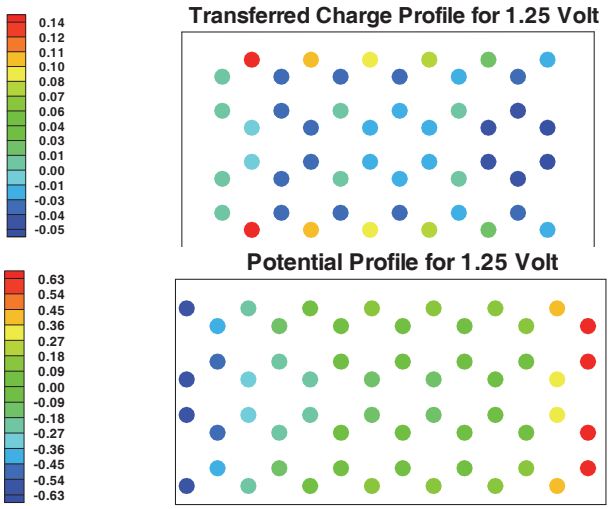

Fig. 14. Transferred charge and Electrostatic potential profiles for $V_{\rm sd} = 1.25$ volt and $V_g = 0.5$ volt in the weak screening case. Due to charge transfer through the ribbon edges, screening is so weak that the external potential can penetrate inside the central portion.

details of the electrostatic potential profile. Because of strong screening in low voltages, the major potential drop takes place at the contacts. However, in voltages larger than the NDR threshold, due to charge transfer through the ribbon edges, screening is so weak that the external potential can penetrate inside the central portion. As a consequence, off current reduces in comparison to non-interacting ribbons.
In addition, e-e interaction enhances on-off ratio of the current which originates from a flat electrostatic potential deep inside the ribbon due to screening of the external bias by electrons close to the junctions. Furthermore, this NDR is not much sensitive to the edge asymmetry. So emerging of this NDR is robust against spin orientation along the edges.

7. References

Novoselov, K. S.& Geim, A. K.& Morozov, S. V.& Jiang, D.& Zhang,Y.& Dubonos, S. V.& Grigorieva, I. V.& Firsov, A. A. (2004). Electric Field Effect in Atomically Thin Carbon Films, In:*Science*, Vol. 306, No. 5696, pp. (666-669).

Liu, Z. & Suenaga, K. & Harris, P. J. F. & Iijima, S. (2009). Open and Closed Edges of Graphene Layers, In:*Phys. Rev. Lett.*, Vol. 102, page. (015501).

Ozyilmaz. B. &Jarillo-Herrero. P. &Efetov. D. & Abanin. D. A.& Levitov. L. S.&Kim. P. (2007). Electronic Transport and Quantum Hall Effect in Bipolar Graphene p-n-p Junctions, In:*Phys. Rev. Lett.*, Vol. 99, page. (166804).

Han, M. Y.& ozyilmaz, B.&Zhang, Y.& and Kim, P. (2007). Energy Band-Gap Engineering of Graphene Nanoribbons, In:*Phys. Rev. Lett.*, Vol. 98, pp (206805).

Molitor, F. &Jacobsen, A.& Stampfer,C.& Güttinger, J.& Ihn, T. and Ensslin, K. (2009). Transport gap in side-gated graphene constrictions, In:*Phys. Rev. B.*, Vol. 79, pp. (075426).

Li, X.& Wang, X.& Zhang, L.& Lee, S.& Dai, H. (2008). Chemically Derived, Ultrasmooth Graphene Nanoribbon Semiconductors, In:*Science*, Vol 319, pp. (1229-1232).

Wang, X.& Ouyang, Y.& Li, X.& Wang, H.& Guo, J.& Dai, H. (2008). Room-Temperature All-Semiconducting Sub-10-nm Graphene Nanoribbon Field-Effect Transistors, In:*Phys. Rev. Lett.*, Vol. 100, pp. (206803).

Son, Y. W.& Cohen, M. L.& Louie, S. G. (2006). Energy Gaps in Graphene Nanoribbons, In:*Phys. Rev. Lett.*, Vol. 97, pp. (216803).

Sols, F. &Guinea, F.& Castro Neto, A. H. (2007). Coulomb Blockade in Graphene Nanoribbons, In: *Phys. Rev. Lett.*, Vol. 99, pp. (166803).

K. Nakada, K.& Fujita, M.& Dresselhaus, G.& Dresselhaus, M. S. (1996). Edge state in graphene ribbons: Nanometer size effect and edge shape dependence, In: *Phys. Rev. B.*, Vol. 54, pp. (17954Ű17961).

Brey, L.& Fertig, H. (2006). Edge states and the quantized Hall effect in graphene, In. *Phys. Rev. B.*, Vol. 73, pp. (195408-195413)

Brey, L.& Fertig, H. (2006). Electronic states of graphene nanoribbons studied with the Dirac equation, *Phys. Rev. B.*, Vol. 73, pp.(235411-235416).

Zheng, H.& Wang, Z. F.& Luo, T.& Shi, Q. W.& Chen, J. (2007). Analytical study of electronic structure in armchair graphene nanoribbons, In: *Phys. Rev. B.*, Vol. 75, pp. (165414-165420).

Malysheva, L.& Onipko, A. (2008). Spectrum of π Electrons in Graphene as a Macromolecule, In: *Phys. Rev. Lett.*, Vol. 100, pp. 186806.

Mucciolo, E. R.& Castro Neto, A.& Lewenkopf, C. H. (2009). Conductance quantization and transport gaps in disordered graphene nanoribbons, In: *Phys. Rev. B.*, Vol. 79, pp. (075407-075412).

Li, Z.& Qian, H.& Wu, J.& Gu, B-L.& Duan, W. (2008). Role of Symmetry in the Transport Properties of Graphene Nanoribbons under Bias, In: *Phys. Rev. Lett.*, Vol. 100, pp. 206802.

Farajian, A. A.& Esfarjani, K.& Kawazoe, Y. (1999). Nonlinear Coherent Transport Through Doped Nanotube Junctions, In: *Phys. Rev. Lett.*, Vol. 82, pp. (5084).

Cresti, A.& Grosso, G.& Parravicini, G. P. (2008). Field-effect resistance of gated graphitic polymeric ribbons: Numerical simulations, In: *Phys. Rev. B.*, Vol. 78, pp. (115433-115440).

Cresti, A.& Grosso, G.& Parravicini, G. P. (2008). Valley-valve effect and even-odd chain parity in p-n graphene junctions, In: *Phys. Rev. B.*, Vol. 77, pp. (233402).

Akhmerov, A. R.& Bardarson, J. H.& Rycerz, A.& Beenakker, C. W. J. (2008). Theory of the valley-valve effect in graphene nanoribbons, In: *Phys. Rev. B.*, Vol. 77, pp. (205416-205421).

Nakabayashi, J.& Yamamoto, D.& Kurihara, S. (2009). Band-Selective Filter in a Zigzag Graphene Nanoribbon, In: *Phys. Rev. Lett.*, Vol. 102, pp. (066803).

Wakabayashi, K.& Aoki, T. (2002). Electrical conductance of zigzag nanographite ribbons with locally applied gate voltage, In: *Int. J. Mod. Phys. B.*, Vol. 16, pp. (4897-4909).

Wang, Z. F.& Li, q.& Shi, Q. W.& Wang, X.& Yang, J.& Hou, J. G.& Chen, J. (2008). Chiral selective tunneling induced negative differential resistance in zigzag graphene nanoribbon: A theoretical study, In: *Appl. Phys. Lett.*, Vol. 92, pp. (133114).

kobayashi, Y.& Fukui, K. I.& Enoki, T.& Kusakabe, k. (2006). Edge state on hydrogen-terminated graphite edges investigated by scanning tunneling microscopy, In: *Phys. Rev. B.*, Vol. 73, pp. (125415-125423).

Niimi, Y.& Matsui, T.& Kambara, H.& Tagami, K.& Fukuyama, H. (2006). Scanning tunneling microscopy and spectroscopy of the electronic local density of states of graphite surfaces near monoatomic step edges, In: *Phys. Rev. B.*, Vol. 73, pp. (085421).

Ren, Y.& Chen, K-Q. (2010). Effects of symmetry and StoneŰWales defect on spin-dependent electronic transport in zigzag graphene nanoribbons, In: *J. Appl. Phys.*, Vol. 107, pp. (044514).

Esaki, L. (1958). New Phenomenon in Narrow Germanium p-n Junctions, In: *Phys. Rev.*, Vol. 109, pp. (603-604).

Dragoman, D.& Dragoman, M. (2007). Negative differential resistance of electrons in graphene barrier, In: *Appl. Phys. Lett.*, Vol. 90, pp. (143111).

Cheraghchi, H.& Esfarjani, K. (2008). Negative differential resistance in molecular junctions: Application to graphene ribbon junctions, *Phys. Rev. B.*, Vol. 78, pp. (085123).

Ulloa, S. E.& Kirczenow, G. (1987). Electronic structure of staging dislocations, electron scattering states, and the residual resistance of graphite intercalation compounds, iN: *Phys. Rev. B.*, Vol. 35, pp. (795).

Jackson, J. D. (1975). *Classical Electrodynamics* (New York: John Wiley and Sons), 2 nd Ed.

Esfarjani, K.& Kawazoe, Y. (1998). Self-consistent tight-binding formalism for charged systems, In: *J. Phys.: Condens. Matter*, Vol. 10, p. (8257).

Ohno, K. (1964). Some remarks on the Pariser-Parr-Pople method , Theor. Chim. Acta. Vol. 2, p. (219); Klopman, G. (1964). A Semiempirical Treatment of molecular Structures. II. Molecular Terms and Application to diatomic Molecules, J. Am. Chem. Soc. Vol. 86, pp. (4550Ű4557).

Nardelli, M. B. (1999). Electronic transport in extended systems: Application to carbon nanotubes, *Phys. Rev. B.*, Vol. 60, pp. (7828Ű7833).

Broyden, C. G. (1965). A class of methods for solving nonlinear simultaneous equations , Math. Comput. Vol. 19, pp.(577-593), also See, e.g., Ohno, K. & Esfarjani, K. & Kawazoe, Y. *Computational Materials Science from Ab Initio to Monte Carlo Methods* (Springer, Berlin, 1999).

Munoz, M. C. *et al.*, (1988). In: *Prog. Surf. Sci.*, Vol. 26, p. (117); Garcia-Moliner F. & Velasco, V. R. *Theory of Single and Multiple interfaces* (World Scientific, Singapore, 1992).

Datta, S. *Electronic Transport in Mesoscopic Systems* (Cambridge U.P, Cambridge, 1995).see chapter 2 and references.

Liang, G. C. & Ghosh, A. W. & Paulsson, M. & Datta, S. (2004). Electrostatic potential profiles of molecular conductors, In: *Phys. Rev. B.*, Vol. 69, pp. (115302).

Ezawa, M. (2006). Peculiar width dependence of the electronic properties of carbon nanoribbons, In: *Phys. Rev. B.*, Vol. 73, pp. (045432).

Rainis, D. & Taddei, F. & Dolcini, F. & Polini, M. & Fazio, R. (2009). Andreev reflection in graphene nanoribbons, In: *Phys. Rev. B.*, Vol. 79, pp. (115131).

Taylor, J. & Guo, H. & Wang, J. (2001). Ab initio modeling of quantum transport properties of molecular electronic devices, In: *Phys. Rev. B.*, Vol. 63, pp. (24540).

Cheraghchi, H.& Esmailzadeh, H. (2010). A gate-induced switch in zigzag graphene nanoribbons and charging effects, In: *Nanotechnology*, Vol. 21, pp. (205306).